AD-A215 893

Optimization of Gaussian Beam Widths in Acoustic Propagation

D. F. Gordon

DTIC
ELECTE
DEC 15 1989
S E D

89 12 14 108

NAVAL OCEAN SYSTEMS CENTER
San Diego, California 92152-5000

J. D. FONTANA, CAPT, USN
Commander

R. M. HILLYER
Technical Director

ADMINISTRATIVE INFORMATION

Released by
E. F. Rynne, Jr., Head
Acoustic Analysis Branch

Under authority of
T. F. Ball, Head
Acoustic Systems and
Technology Division

FS

REPORT DOCUMENTATION PAGE

Form Approved
OMB No. 0704-0188

1 AGENCY USE ONLY (Leave blank)	2. REPORT DATE October 1989	3. REPORT TYPE AND DATES COVERED Final

4 TITLE AND SUBTITLE OPTIMIZATION OF GAUSSIAN BEAM WIDTHS IN ACOUSTIC PROPAGATION	5. FUNDING NUMBERS PE: 0602314N WU: DN308 105
6 AUTHOR(S) D. F. Gordon	

7 PERFORMING ORGANIZATION NAME(S) AND ADDRESS(ES) Naval Ocean Systems Center San Diego, CA 92152-5000	8. PERFORMING ORGANIZATION REPORT NUMBER NOSC TD 1678

9 SPONSORING/MONITORING AGENCY NAME(S) AND ADDRESS(ES) Office of Naval Technology Arlington, VA 22217	10. SPONSORING/MONITORING AGENCY REPORT NUMBER

11 SUPPLEMENTARY NOTES

12a. DISTRIBUTION/AVAILABILITY STATEMENT Approved for public release; distribution is unlimited.	12b. DISTRIBUTION CODE

13. ABSTRACT (Maximum 200 words)

This report outlines a beam-width minimization technique applied to a Gaussian beam model.

Accession For

NTIS GRA&I ☒
DTIC TAB ☐
Unannounced ☐
Justification

By
Distribution/
Availability Codes

Dist | Avail and/or Special

A-1

14 SUBJECT TERMS gaussian beams beam widths	15. NUMBER OF PAGES 22
	16. PRICE CODE

17 SECURITY CLASSIFICATION OF REPORT UNCLASSIFIED	18 SECURITY CLASSIFICATION OF THIS PAGE UNCLASSIFIED	19 SECURITY CLASSIFICATION OF ABSTRACT UNCLASSIFIED	20 LIMITATION OF ABSTRACT

CONTENTS

FIGURES

1.0 INTRODUCTION

The use of Gaussian beams to compute wave propagation phenomena is a field of current interest and activity. Porter and Bucker (1987) supply an extensive list of references. More recent references can be found in Benites and Aki (1989). Gaussian beams can be traced as rays in range-dependent media providing not only propagation loss, but travel times, multipath structure, and frequency dependence. The well-known ray theory problems of caustics and shadow zones are treated automatically.

This report outlines a beam width minimization technique applied to a Gaussian beam model developed by Dr. H. P. Bucker. Porter and Bucker (1987) gives the formulation upon which the technique is built. A free parameter E (called ϵ in Porter and Bucker, 1987) is usually determined in a heuristic manner. Here, it is shown that the minimization of beam width assigns a precise value to E. Examples are given showing that the minimized beams give good propagation losses in some cases.

A case is also shown in which the standard Gaussian beams give poor results and the minimized beams give even worse results. The problem appears to arise in beams that pass near boundaries. This problem will have to be corrected before a final judgment can be made on the validity of minimum-width beams.

Gaussian beam cross-sectional intensities and curvature are controlled by two functions, p and q. Several examples of these functions are plotted in this report and their nature is clarified.

In section 2.0 of this report the parts of Gaussian beam theory used here are reviewed. The following sections then discuss the beam minimization and show examples.

2.0 REVIEW OF GAUSSIAN BEAMS

The Gaussian beam theory and notation used here is that reported by Porter and Bucker (1987). In this section some equations from Porter and Bucker (1987) that are used in later sections will be presented.

A Gaussian beam is assumed to have the form

$$w(s, n) = A(s, z) \; exp \; \{ - i\omega \; [\; t(s) \; + \; Bn^2 \;] \; \}, \tag{1}$$

where w is the sound pressure, s is the arc length along a ray, n is the normal distance from the ray, z_o is the depth of the point source, ω is the angular frequency, and t is the travel time along the ray. Thus, the Gaussian beam in the current view is inseparably tied to ray theory. The center of the beam is a ray which defines s and t; the field u at a point in space is determined by the minimum distance, n, from the central ray.

The parameter B is a complex number. The imaginary part defines the rate at which the beam acoustic pressure decreases from the center, or equivalently defines

1

the beam width. This imaginary part of B must be negative if the beam is to decrease away from the center. This is assumed to be a physical requirement at all times.

The real part of B adds to the travel time to determine the acoustic phase at a point removed from the central ray. If this real part of B is zero, there is no phase change perpendicular to the beam and the beam has the phase behavior of a plane wave. Near a point source the wave fronts are expected to be circles (in two dimensional representations) so the phase increases in directions perpendicular to the central ray. Therefore, the real part of B must be positive near the point source. The beam does not have to maintain this convex curvature at all ranges and, in fact, in convergence zone propagation often becomes concave.

The central problem in utilizing the beam as in equation (1) is to determine the parameter B at any given point along the ray. Porter and Bucker (1987) give a derivation and cite further references. In general, the behavior of rays near the central ray when constrained by the Gaussian condition of equation (1) must be determined and expressed in the ray dependent, (s, n) coordinate system. Rays near the central ray might differ from it slightly because of a different ray parameter or because of a different source point. Thus, a variation in two parameters should provide the real and imaginary parts of B.

Porter and Bucker express B as the ratio of two functions $p(s)$ and $q(s)$, or

$$B = (p/q)/2. \tag{2}$$

They then show that p and q can be computed by integrating the following set of differential equations along the ray:

$$dq/ds = C(s)p(s),$$
$$dp/ds = -C_{nn}(s)q(s)/c^2(s), \tag{3}$$

where C is the sound speed and C_{nn} is the second partial derivative of the sound speed in the normal direction.

The field of a point source can now be expressed in an asymptotic expansion and compared to a Gaussian beam sum to evaluate A in equation (1). The value of A appropriate for a point source is found to be

$$A = \delta a \; exp(i\pi/4) \, [C(s)q(o)\omega \; cos \; a/2 \; \pi \; rq(s)]^{1/2}/C_o , \tag{4}$$

where a is the angle from the horizontal to the beam center at the source and δa is the separation between adjacent beam angles. The sound speed C and q are evaluated at the source and at the arc length s.

The usual application of equations (1), (2), and (4) is to launch equally-spaced beams from the source. The distance n is then the closest approach of the beam center to the receiver point. The point on the center ray that is closest to the receiver determines the ray length s. At this point the receiver is on the perpendicular to the ray.

A beam will contribute to any receiver, although a distance between beam and receiver can usually be found where the beam contribution is negligibly small. The field at a given point will usually consist of contributions from a number of beams that are sufficiently close to the receiver. If the beams can be made narrower, fewer beams will contribute to a given receiver point. This depends upon p/q and their starting values.

For the present let

$$p(0) = 1 \text{ and } q(0) = iE_o . \tag{5}$$

The function p starts at a real number and q starts with a pure imaginary constant E_o. Following Porter and Bucker (1987), in a medium with constant sound speed C, the rays are straight lines and equation (3) gives

$$p(s) = 1 \text{ and } q(s) = C_0 s + iE_o , \tag{6}$$

because C_{nn} is zero. Thus, in a uniform medium the beam width will depend upon the starting value E_o near the source but at long distances from the source (large s) will become approximately proportional to s. When $C_0 s = E_o$, the two terms have about equal effect. This cross-over point will turn out later to be related to the optimum beam width.

3.0 OPTIMIZATION OF BEAM WIDTH

Porter and Bucker (1987) suggest values of E_o as starting values for q. These are functions of the beam spacing δa and make the beams overlap at their $1/e$ down points in the far field. These, and similar values of E_o, were tried in a convergence zone environment. It was found that similar sound fields were computed no matter what value of E_o was used. Any selected E_o resulted in values of p and q, and therefore values of A and B which gave a similar value for the acoustic field. Propagation losses were generally within 3 dB of each other. These observations led to a closer examination of the functions p and q, and to the concept that E_o could be chosen independently for each beam and was not a true constant. The subscript o will therefore be omitted from E when used in this context. Observation showed that p and q could be written as

$$p = a + iEb,$$

and

$$q = c + iEd. \tag{7}$$

Thus, the real parts of p and q are independent of E, and the imaginary parts remain directly proportional to E as p and q are integrated along the ray. These follow from equations (3) and (5) because C, C_{nn}, and E are real numbers.

One implication of equation (7) is that E does not have to be determined at the start of a beam calculation. It can be set to 1 and then when the beam contributions at a field point are evaluated, an appropriate value of E can be selected.

A second implication is that if the initial values of both real and imaginary parts were in p and both parts of q were zero, then identical functions for real and imaginary p and q would be obtained differing only by a constant factor. Starting p real and q imaginary as in equation (5) is a method for obtaining two independent solutions that can determine both beam width and beam curvature.

Figure 1* shows p and q for a specific ray and illustrates the previous points. The ray in the upper panel leaves the source at 1000-m depth at an angle of 4.3° from horizontal where positive ray angles are downgoing. The sound-speed profile used here is the Munk-canonical profile with the axis of minimum sound speed at 1300-m depth. The profile is shown in Porter and Bucker (1987), figure 6. The scales on p and q apply only to the real parts, since the imaginary parts are proportional to E. For reasons to appear later, E is assumed to be negative. In general, on this and similar figures to follow, the shape of the curves and not the actual excursions are important. Units are given for q under the assumption that imaginary q is a second independent solution with the same units as real q, and p is unitless. The magnitude of q is about 10^7 larger than p.

Figure 1 shows that the parts of p and q are almost cyclical functions of range (and ray length s). This follows from equation (3) because convergence zone profiles have generally positive second derivatives C_{zz} of sound speed with depth, and convergence zone rays have shallow angles so C_{nn} is close to C_{zz}. This behavior of p and q can be contrasted with that of equation (6) for constant sound speed.

Figure 2 also shows the ray and p and q, this time for the upgoing ray of –4.3° at the source. Figure 3 shows the same quantities for a downgoing ray of 8.6°. This ray, traveling farther from the sound speed axis, is effected by more extreme values of C_{nn}.

These figures make it clear that p and q express the effects of ray refraction upon the beam parameters, while E is a free parameter that might be used to optimize the beam parameters. The most apparent optimization, and the one used here, is to minimize beam width. From equation (1), this means the imaginary part of B, therefore of p/q, must be as large negatively as possible. To this end, p/q is expressed in terms of equation (7) giving

$$p/q = (ac + E^2 bd)/y^2 + iE(bc - ad)/y^2 , \qquad (8)$$

where

$$y^2 = c^2 + E^2 d^2 .$$

---

*Figures in this report are combined at the end of text.

4

The imaginary part of p/q is now differentiated and set equal to zero giving

$$E = \pm \ (c/d)^{\ 1/2} \ . \tag{9}$$

The choice of sign must make the imaginary part of p/q negative. Therefore, the sign of E will be chosen opposite to the sign of the term *(bc - ad)* from equation (8). This term has been observed to be almost constant along a ray, or for the starting values of equation (5) is almost $-E_o$. This is the reason imaginary q was started as a negative number in figures 1 through 3, and is consistent with the minus sign in equation (1).

Substituting equation (9) into equation (8), the optimized value for p/q is

$$(p/q)_{opt} = (a/c + b/d)/2 - i|b/d - a/c|/2 \ . \tag{10}$$

The second term is negative when the sign of E is selected. The first term of equation (10) is undefined at zero range. However, at a small distance along the ray, figures 1, 2, or 3 show a/c is a large positive number while b/d is a small negative number. (The large size of q compared to p does not change the relative sizes.) At this small distance, the first term of equation (10) is positive as is the travel time. As discussed in section 2.0, this ensures convex curvature near the source.

The effect of equation (9) on q is to make the real and imaginary parts equal except for sign. For example, if figure 1 were the optimized p and q, the imaginary part of q would be multiplied by a different E at each range to keep its magnitude equal to that of real q. However, the sign remains the same. At the range where imaginary q crosses zero, E becomes infinite and the optimized imaginary q will jump from the opposite sign of real q to the same sign or vice versa.

When real q in figure 1 goes through zero, E simply becomes zero and so does the optimized imaginary q. These points are apparently the caustic points of ray theory. This is indicated by examining ray diagrams. Figure 4 is a portion of the ray diagram of figure 7 from Porter and Bucker (1987). The rays of figures 1 and 2 can be identified by the depths of their apexes near 735 m. The downgoing ray touches the caustic near 37 and 53 km; the upgoing near 52 km. These are the zero crossing points of real q in figures 1 and 2.

These caustics are equivalent to the zeros of c in equation (10), and p/q is infinite. Thus, the beam collapses to zero width at the caustic. Any receiver point more than an infinitesimal distance off the center of the beam will have zero intensity. Near the caustic the beam will be narrow, but intense. The intensity follows from the term A of equation (4).

At the zeros of imaginary q or $d = 0$, the beam again reaches zero width and infinite intensity. There is no evidence of caustics here. Apparently, the optimization of beam width is not limited at these points, and values of E are permitted that bring the beam to zero width. However, the user is not required to select the optimum E and an upper bound can be put on the magnitude of E in a program.

5

In between the two types of critical points discussed above, the optimized beam spreads to larger widths. The width will remain finite because the two parts of p, a, and b of equation (10) will not become zero at the same time permitting p/q to be zero. The plots of p in figures 1 through 3 suggest that the zeros will be separated.

4.0 PROGRAMMING CONSIDERATIONS

In this section some techniques used in the Gaussian beam propagation-loss program written by H. P. Bucker are discussed with consideration to optimizing beam width and some results are presented.

Central rays are computed including travel time with Runge-Kulta type integrations. Steps in s of 100 or 200 m are usually used. Equation (3) for p and q are integrated simultaneously. E_o is set to one. These somewhat computer-time intensive methods permit range-dependent sound-speed variation, though that is not the case here. As beam centers are traced near receivers, the distances to the receivers are calculated at each step to find minimums. When the presence of a minimum is indicated, the true minimum is determined by interpolation and s, n, t, p, q, and E are evaluated. If desired, the magnitude of E is checked and limited.

The method used to limit E may be more cautious and computer time consuming than necessary. The maximum magnitude of both parts of q that has been encountered along the beam is saved and updated at each step. When an E is computed it is limited to 10 times the ratio of maximum-real q and maximum-imaginary q. This cautious method is used because the behavior of q, illustrated in figures 1 through 3, has not been observed for enough different acoustic ducts and the limits on its excursions are not known.

When the required parameters have been determined for the point on the beam center closest to the receiver, the acoustic pressure is determined by equation (1), using the optimized values of p and q. Care must be used in taking the complex square root in A in equation (4). The square root must be multiplied by $(-1)^k$, where k is the number of times the argument has crossed $180°$. This number is determined by keeping track of zero crossings of imaginary q as the beam center is being integrated. If the square root of $q(s)$ is taken by itself, the above determination of k will work. However, if a single square root of the entire argument is used then $q(0)/q(s)$ determines the phase in the complex plane. The square root branch line occurs when $q(s)$ crosses $270°$ since $q(o)$ is a negative imaginary constant.

An even more careful treatment of the above process is required if occasional errors are to be avoided. The zero crossings of q are determined at the end of each step in s along the central ray. The actual crossing occurred at some point along the last ray segment. If a point of minimum distance to a receiver also occurs in this segment, it is necessary to determine on which side of the zero crossing the receiver point lies. An alternative treatment is to interpolate the square root of q from square roots at either end of the segment that have been corrected for their appropriate number of zero crossings.

6

5.0 EXAMPLES

Three examples are given here. An example of a deep source and receiver, well removed from boundaries gives an excellent prediction of propagation losses. A shallow receiver example shows significant differences between Gaussian-beam results and normal-mode results. Finally, an example of the sequence of acoustic pressures at a receiver for a family of beams is shown.

Figure 5 compares the first convergence zone for a 1000-m source and 800-m receiver at 50-Hz frequency. This is the same case as illustrated in Porter and Bucker (1987), figure 8. The Munk-canonical profile is used. There are minor differences between the sound-speed profiles here because the normal-mode program was limited to 12 layers. The normal mode profile from 3000 to 5000 m is represented by a single layer, while the Gaussian-beam profile uses four layers. The Gaussian-beam profile has a reflective bottom but beams were limited to those whose center cleared the bottom. The normal-mode bottom was lossy (a negative gradient half space).

In figure 5 the disagreement beyond 65 km is probably due to the different bottom treatments. The most serious disagreement is near the caustic at 40 km. The noticeable disagreement near 54 km is probably due to the nearby caustics at 52 and 53 km.

The inexact losses near caustics should not be viewed as serious. Considering the extensive measures that extended ray theories must use to handle caustics, the results here, achieved with no change in algorithm near the caustic and no requirement to locate the caustic, are very encouraging.

The differences in the Gaussian beam results of figure 5 and those of Porter and Bucker (1987), figure 8 have not been investigated. How much is due to using optimized beam widths and how much to other variables is not known. Here, beam spacing of 0.66° and ray step lengths of 200 m were used.

Figure 6 is propagation loss for a 300-m source and 150-m receiver. Other parameters are the same as for the previous case. The points on the figure will be used later. The Gaussian beam losses are obviously in error. The beams all pass near the surface and the bottom. The interaction of the skirts of the beams with these boundaries is a likely source of the error. However, this has not been fully investigated at this time.

Figure 7 shows the location of the centers and the pressures of some of the Gaussian beams that contribute to the receiver in figure 6 at 61-km range and 150-m depth. These points are the points on the central ray at the point closest on the ray to the receiver. These are also the points at which the receiver is on the normal to the ray. The beam spacing is 0.33°, and every other beam is generally plotted. The numbers on the plot give angles of the beam centers at the source.

The two lower panels show the acoustic pressure of the beams as loss in decibels. The upper and lower of these two panels refer to the upper and lower parts of the trace in the depth-versus-range plot above. The pressures also have phase which is not represented here.

7

For comparison, corresponding pressures for a conventional Gaussian beam treatment are shown in figure 8. A constant value of E of 1.09×10^7 is used for all beams. The most obvious difference in the standard- and optimized-beam width is near the caustic or beams where real q goes through zero at a source angle of $2.3°$. This is at the left-hand edge of the plots. These beams, when beam width is minimized, contribute little to the receiver 600-m distant, but contribute as strongly as any when beam width is not minimized as in figure 8. Another caustic occurs at $-5.9°$ source angle. It is followed by a zero in imaginary q at $-6.0°$. These produce the somewhat confused pressures near the center of the lower panel in figures 7 and 8. At source angles greater than $10.3°$, the rays are surface reflected.

The individual beam pressure as represented in figures 7 and 8 add up to 92.3 and 85.8 dB, respectively. This is a considerable difference and the smaller loss of the traditional beams is much closer to the desired answer. To see if the problems indicated in figure 6 are due to the beam optimization process, the loss of each kilometer was computed with traditional beams and are plotted as points on figure 6. These losses are definitely in better agreement with the mode theory than are the optimized beam losses. However, the agreement is poor enough to indicate a problem. Beams that pass near the bottom and the surface are probably still the problem. The optimized beams are obviously more susceptible to this problem.

This particular case is unusual in that all beam centers pass near boundaries but only an insignificant few actually reflect from the surface. Upon reflection, p and q are modified as indicated in Porter and Bucker (1987) to accommodate beam reflections. This case forces attention on a remaining problem for Gaussian beams. Two solutions are possible. First, p and q could be modified as the central ray passes near a boundary giving a partial boundary effect. Second, the part of the beam skirt that actually touches the boundary could be modified when it supplies the acoustic field at a receiver further along the beam. In this second case the cross section of the beam will become nonsymmetric. Neither solution has been investigated to date by the author.

6.0 SUMMARY

The use of Gaussian beams to compute underwater sound fields from a point source has been reviewed, using the method reported by Porter and Bucker (1987). A method of minimizing beam width was then developed. An advantage of this method is the elimination of a free parameter, E, that has been a problem in previous implementations.

Propagation-loss plots for a normal-mode model and the above Gaussian-beam method were compared. For a deep source and receiver, well removed from boundaries, the comparison was good. However, for a shallow source and receiver the Gaussian beams give poor results. Arguments are made that the problem is caused by beams whose centers pass near the surface and the bottom. Because of their width the beams should be effected by the surface and bottom. The current theory does not include such effects.

An example of the acoustic pressures at a receiver contributed by each beam is shown. This succession of pressures show that many beams contribute to the total pressure at a receiver, even when beam widths are optimized.

7.0 RECOMMENDATIONS

Gaussian-beam methods are effective for computing propagation loss. They have the flexibility of ray theory but overcome the problems of caustics and shadow zones. However, certain boundary problems remain. Beams that pass near reflecting boundaries but whose centers do not touch should be investigated. Theoretical derivations should be made if not available in the literature, and then tested in existing propagation models.

Once the boundary problems are corrected, the beam width optimization of this report should be tested more exhaustively.
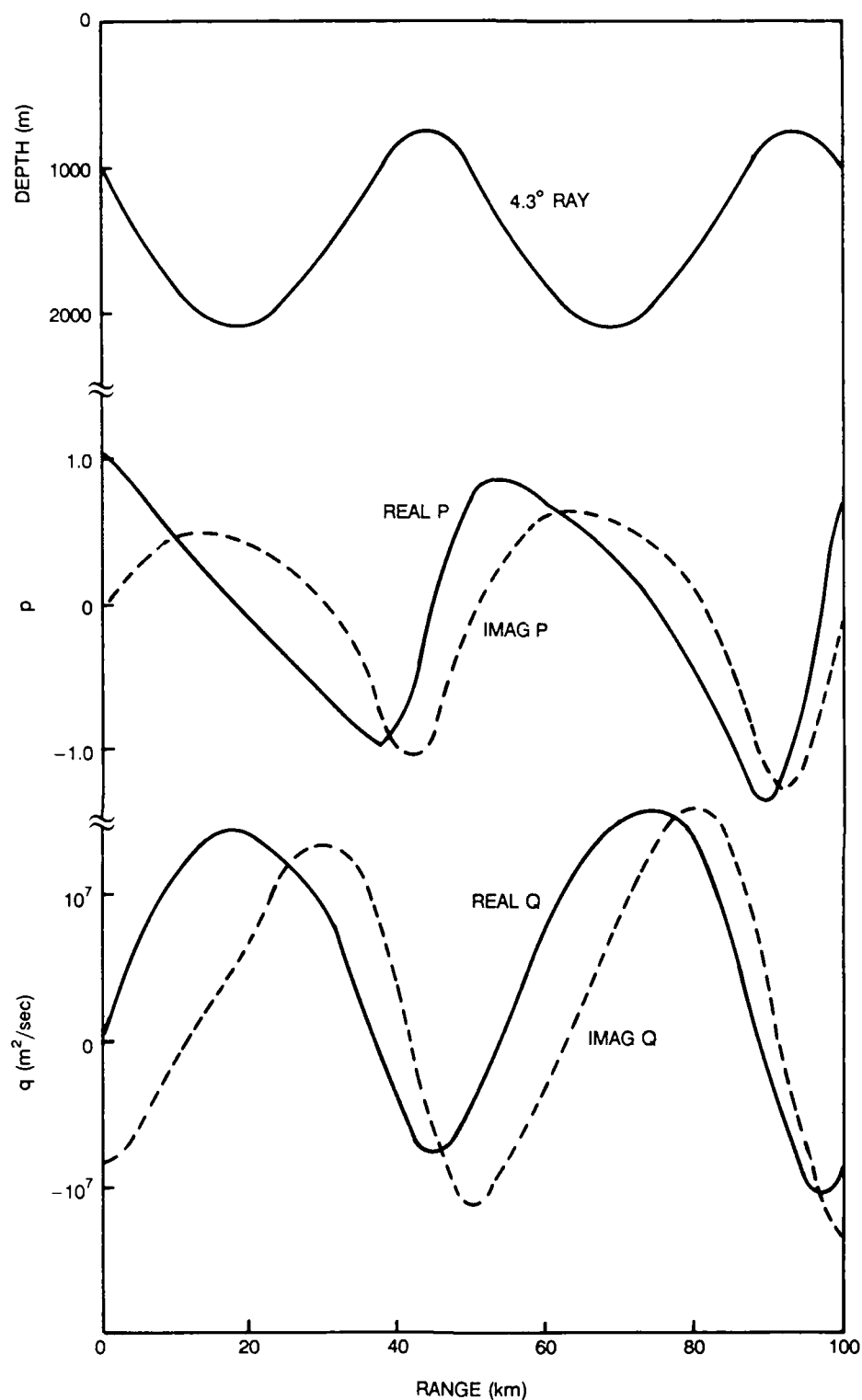
Figure 1. A ray path having the source at 4.3° below the horizontal with the corresponding values of beam functions *p* and *q*. Both real and imaginary parts are shown. The ordinates of both imaginary *p* and *q* are arbitrary, being chosen here to match their counterparts.
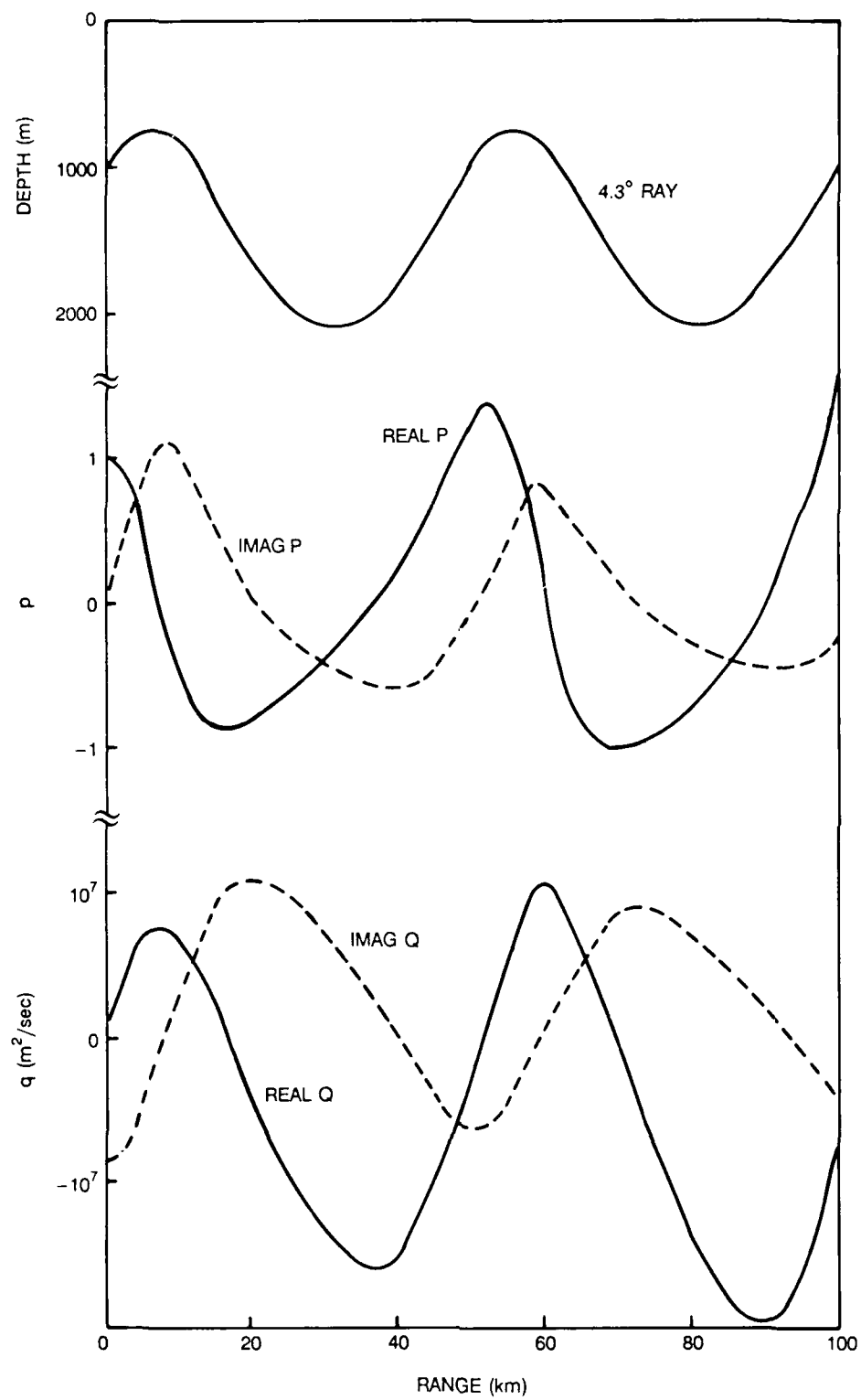
Figure 2. A ray path leaving the source at 4.3° above the horizontal with corresponding values of beam functions *p* and *q*.
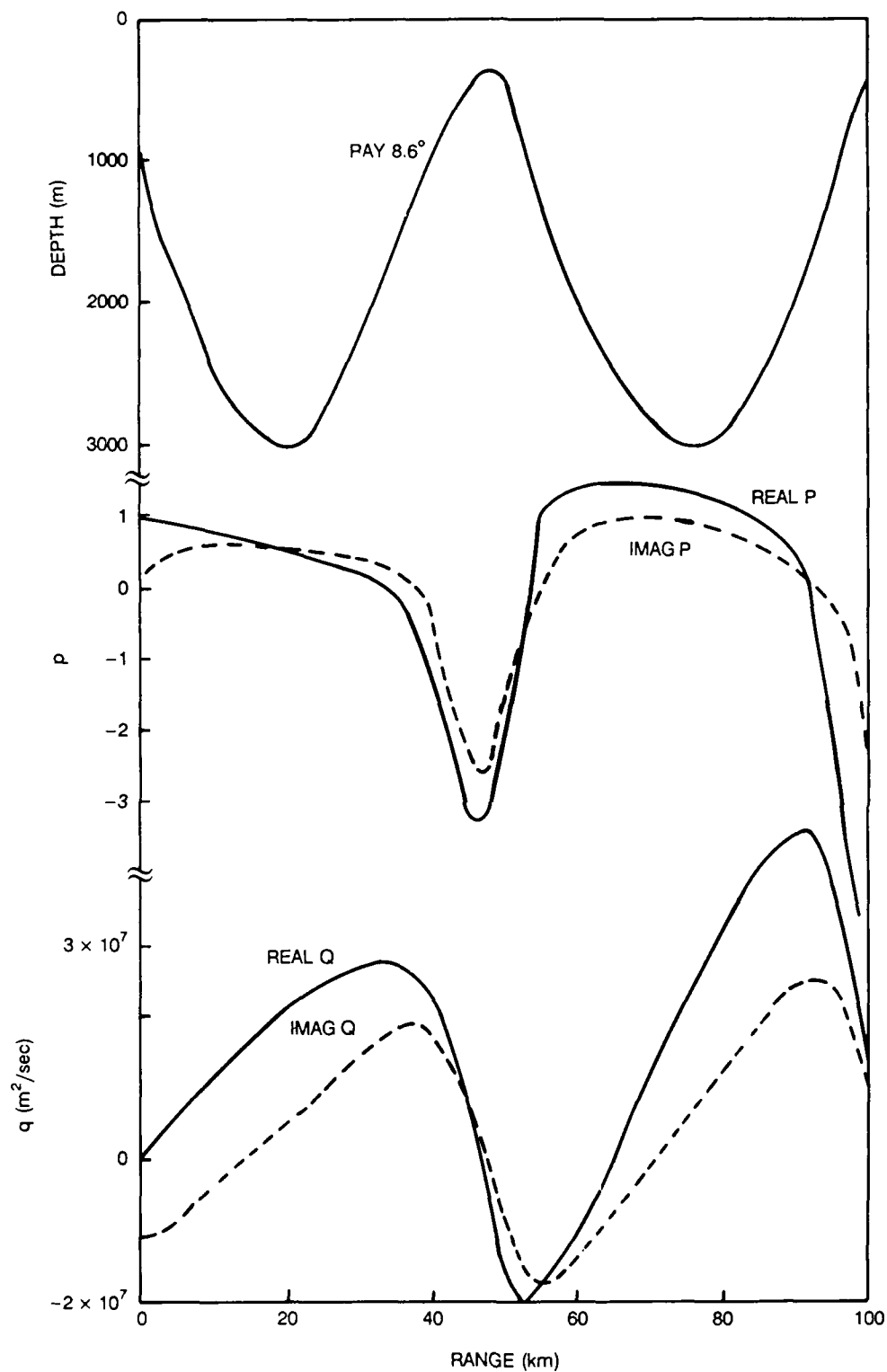
Figure 3. A ray path leaving the source at 8.6° below the horizontal with corresponding value of beam functions *p* and *q*.
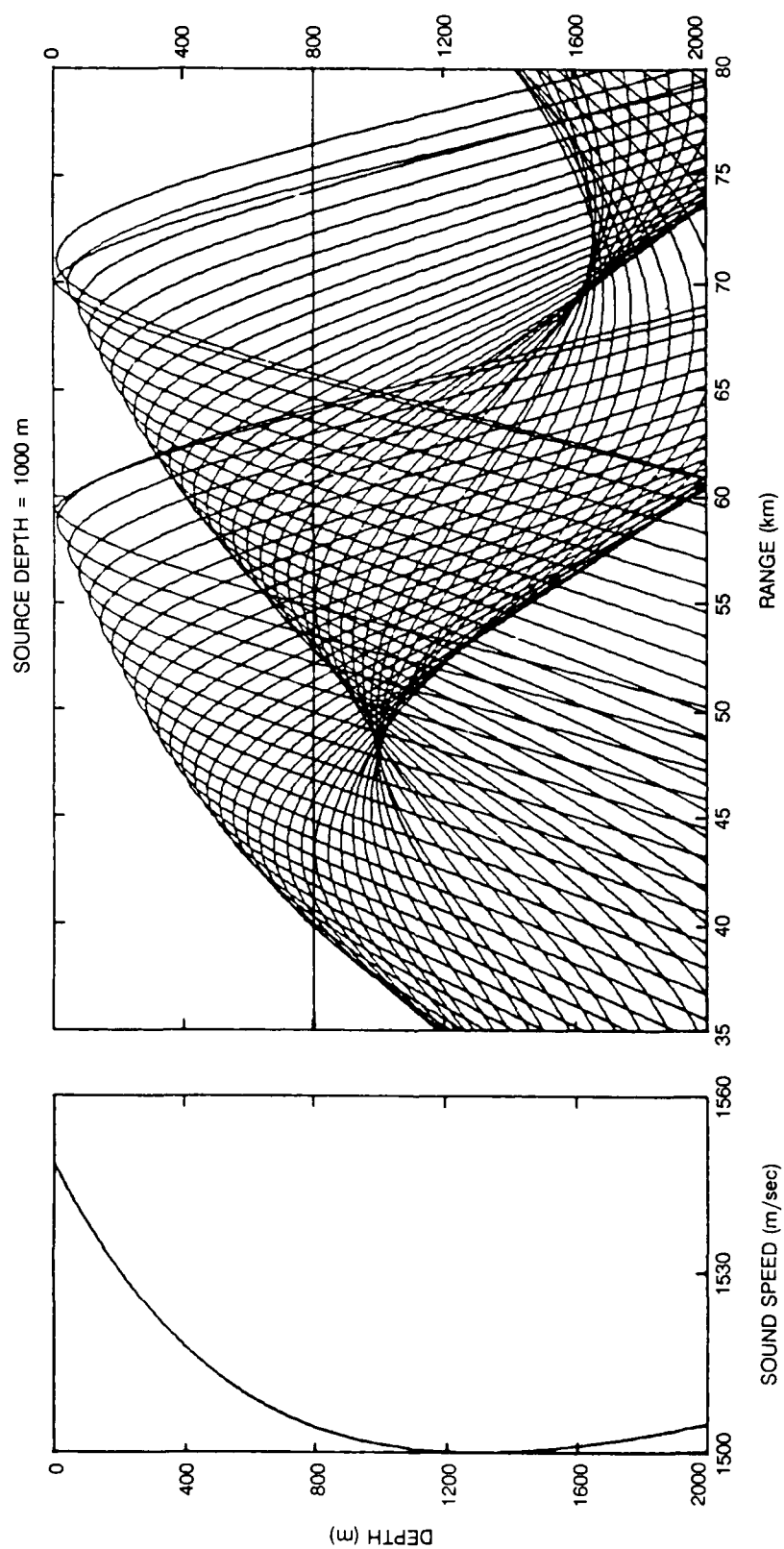
12

Figure 4. Rays from a 1000 m-deep source in a Munk canonical sound-speed profile. Convergence zone 1 is shown.
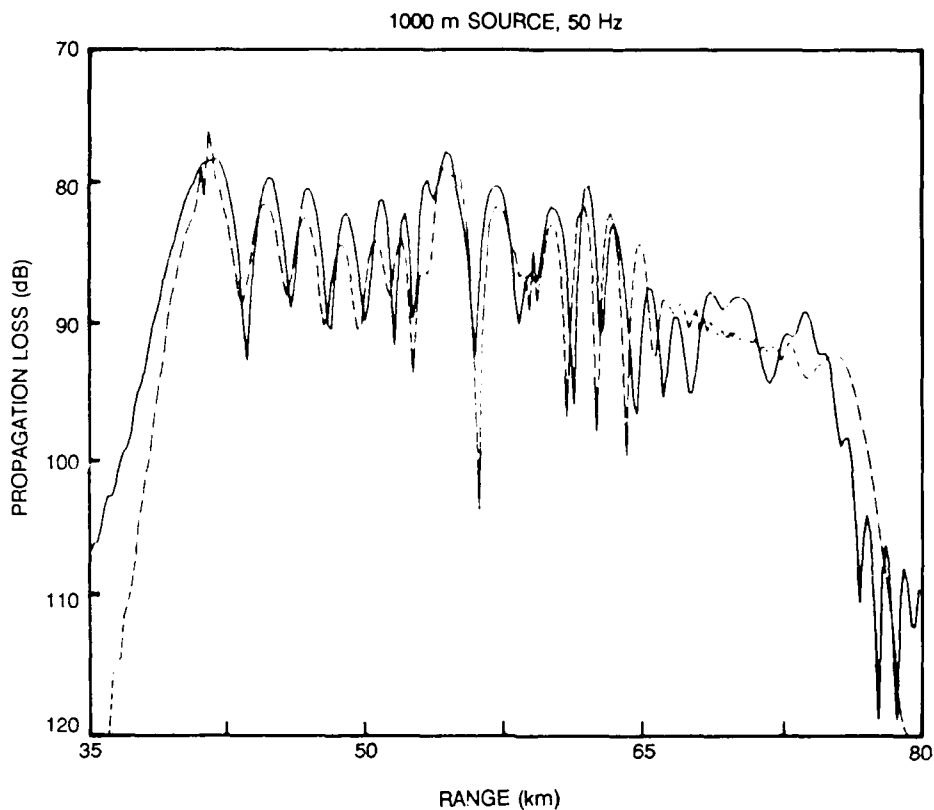
13

Figure 5. Comparison of propagation losses for a 100-m source and 800-m receiver at 50 Hz as computed by a normal-mode model (solid line) and a Gaussian-beam model (broken line).
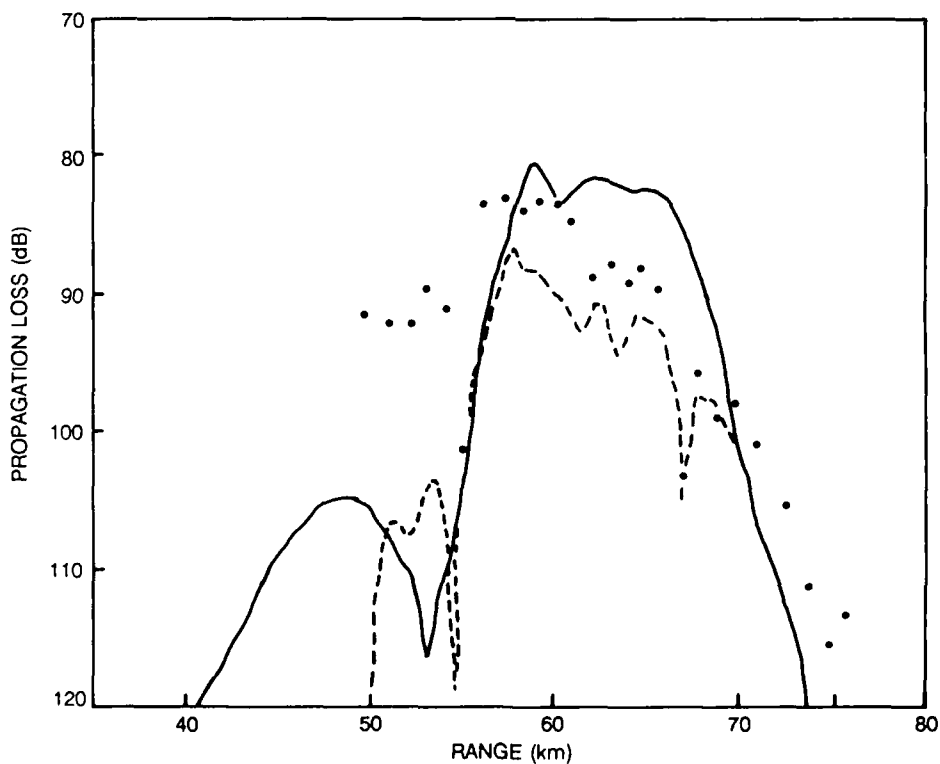

Figure 6. Comparison of propagation losses for a 300-m source and 150-m receiver at 50 Hz. Normal-mode model (solid line), Gaussian beams with minimized widths (broken line), standard Gaussian beams (points).
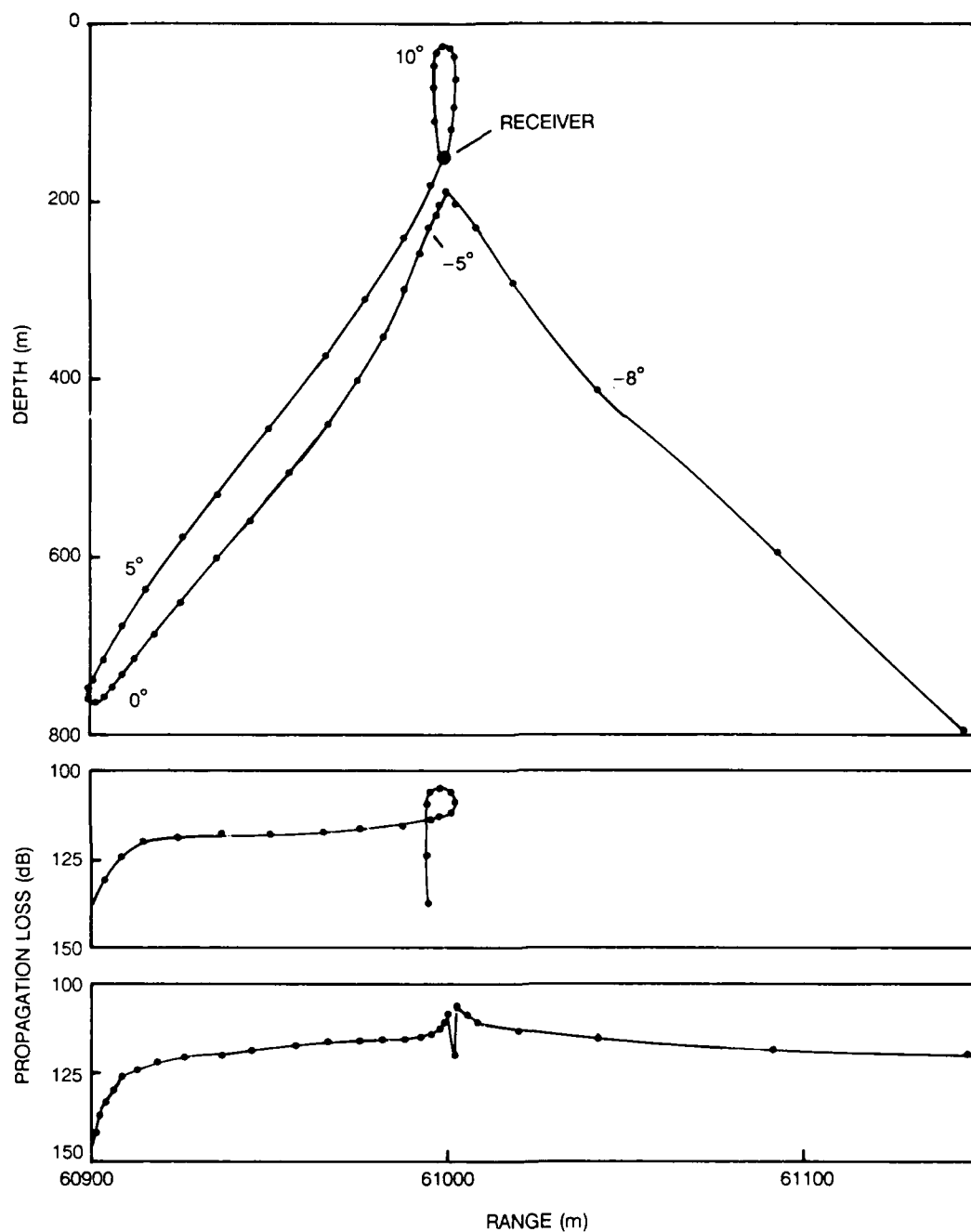
14

Figure 7. Location of beam centers at points perpendicular to the receiver at 150-m depth, 61-km range. Some individual beam positions are shown by points. Absolute value of acoustic pressures at the receiver for the beams whose centers are shown above are shown in the lower two panels as propagation losses.
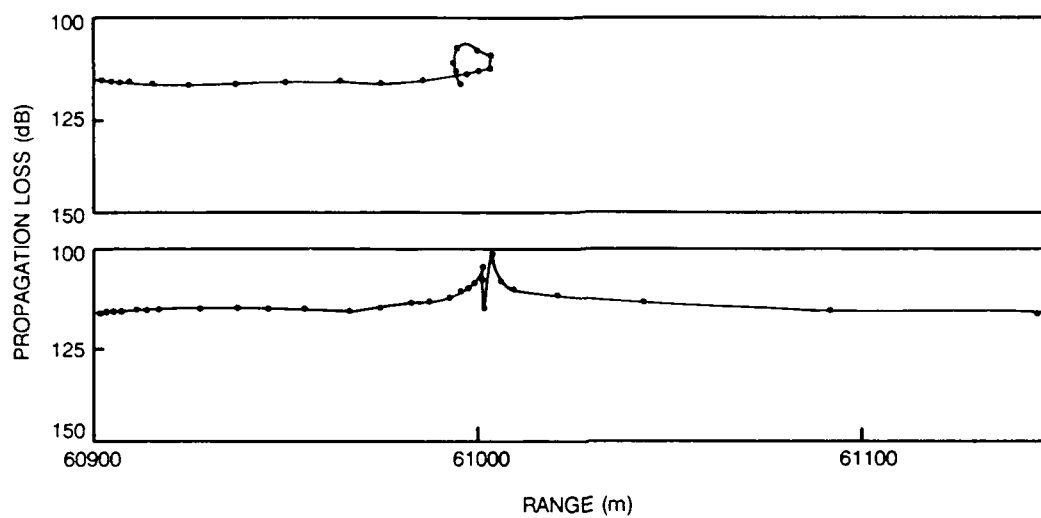
Figure 8. Sound pressures of beams as in figure 7 but for standard beams with constant E.

16

REFERENCES

Porter, M. B. and H. P. Bucker. October 1987. "Gaussian Beam Tracing for Comput-
ing Ocean Acoustic Fields," *J. Acoust. Soc. Am. 82*, 1349-1359.

Benites, R. and K. Aki. July 1989. "Boundary Integral-Gaussian Beam Method for
Sciemic Wave Scattering: SH Waves in Two-Dimensional Media," *J. Acoust. Soc.
Am. 86*, 375-386.

17